

## Numerical investigation of Maxwell Hybrid Nanofluid flow with polystyrene oil as base fluid

Muhammad Bilal,<sup>1, a)</sup> Yasir Mehmood,<sup>2</sup> and Tabinda Shaheen<sup>2</sup>

<sup>1)</sup>Department of Physical Sciences, University of Chenab, Gujrat, Pakistan

<sup>2)</sup>Department of Mathematics, University of Lahore, Sargodha Campus, Pakistan

**ABSTRACT:** This study investigates the thermal enhancement of nanofluids, specifically graphene oxide (GO)/polystyrene and a hybrid nanofluid made of GO + silver (Ag)/polystyrene, over a stretched sheet in porous media under an applied magnetic field. The analysis considers thermal dissipation, convective boundary conditions, heat sources, and wall-to-wall mass transpiration. A non-Newtonian Maxwell fluid is considered. An activation energy impact is also considered for the stagnation point flow over the sheet. Using a Runge-Kutta technique in MATLAB, the shooting method is applied for the flow and heat transfer phenomena to examine the impact of varying key parameters. Results show that higher magnetic field and porosity resistances slow the fluid motion and increase the temperature. Additionally, silver content improves heat transfer efficiency when compared with graphene oxide. This work highlights hybrid nanofluids as effective heat-transport agents with potential industrial applications, especially under natural convection conditions, due to their enhanced thermal properties compared to standard fluids.

---

**Received:** 26 November 2024    **Accepted:** 14 January 2025

**DOI:** <https://doi.org/10.71107/5ecm2g51>

---

### I. INTRODUCTION

Efficiency in heat transport is one of the most critical requirements in modern industrial applications. Traditional cooling agents often fall short of meeting the demands of emerging industries. Nanofluids, containing nano-sized particles (less than 100 nm) dispersed in base fluids such as water, oil, ethylene glycol, polystyrene, or kerosene oil, have shown great promise as effective heat transport agents. The thermal performance of nanofluids has been significantly enhanced through mechanisms such as Brownian motion, heat diffusion, thermophoresis, and the inclusion of nanoparticles. Among these, graphene oxide (GO) in polystyrene and hybrid nanofluids like GO + silver (Ag) in polystyrene have demonstrated exceptional heat transfer capabilities, making them ideal candidates for advanced thermal management systems. The global energy crisis is directly linked

to global warming and environmental degradation. Engineers and scientists continually explore innovative energy solutions to address these challenges and promote sustainability. Among recent advancements, the development of nanoparticles has proven to be highly effective in enhancing the thermal performance of nanofluids. Nanomaterials, widely used as coolants in physical, chemical, and industrial applications, have gained prominence due to their ability to optimize heat and mass transfer processes.

Liquid cooling, a critical factor in various commercial applications, is achieved by dispersing micron-sized nanomaterials into conventional base liquids. These nanofluids are extensively used in refrigeration, air conditioning, and food processing, offering improved efficiency and performance. Some recent research on the flow of nanofluid/hybrid nanofluid over the sheet is highlighted in the following articles<sup>1-9</sup>. From these articles, it is observed that the flow through the stretching sheet in the presence of non-Newtonian Maxwell fluid along with activation energy is still missing. Polystyrene is a kind of fluid that exhibits the characteristics of Maxwell fluid.

Activation energy represents the minimum energy necessary to initiate a chemical process within a system. In nanofluid research, nanoparticles are incorporated into fluid models, where activation energy plays a crucial role in triggering chemical reactions that facilitate the movement and behavior of nanomaterials in

---

<sup>a)</sup>Electronic mail: [mbilal@psh.uchenab.edu.pk](mailto:mbilal@psh.uchenab.edu.pk)

the system. The concept of "activation energy" was introduced by Arrhenius in 1889. Its significance in chemical engineering, geothermal systems, and oil storage industries has made it a fascinating area of study for researchers. The behaviour of a nanofluid made up of water-suspended aluminium alloy nanoparticles was examined by Rekha et al.<sup>10</sup>. By including aspects like activation energy and porous materials in the modelling process, their study concentrated on how a thermal sink/source affected the flow of nanofluids via several geometries, including a wedge, cone, and plate. Ullah et al.<sup>11</sup> used Prandtl-Eyring nanomaterials to represent convective flow on a stretched surface. Their research demonstrated the important effects of activation energy, Joule heating, and chemical reactions in addition to the thermal impact of melting conditioned particles. The effects of chemical reactions and activation energy in a time-dependent mixed convective flow over an infinitely long end-layer were studied theoretically by Dhlamini et al.<sup>12</sup> who also examined the effects of viscous dissipation, Brownian motion, and thermophoresis on temperature, fluid momentum, and chemical species concentration. Non-linear thermal radiative effects in Walter-B nanofluids in a stagnation point flow were investigated by Ijaz Khan and Alzahrani<sup>13</sup>. Their study examined random motion, thermophoresis, and modest magnetic forces that gave the fluid electrical conductivity. Scientists also investigated the effects of chemical reactions, activation energy, and Joule heating to learn more about the fundamental mass and heat transmission mechanisms.

This research investigates the performance of hybrid nanofluids and stagnation point flow towards a stretching sheet, incorporating factors such as heat sources, slip conditions, magnetic field effects, and activation energy. The study considers graphene oxide (Go) and silver (Ag) hybrid nanoparticles in combination with polystyrene as the base fluid. By applying a similarity transformation, the governing partial differential equations (PDEs) with associated boundary conditions are converted into a sys-

tem of nonlinear ordinary differential equations (ODEs). The resulting equations are solved numerically using the shooting method.

## II. PHYSICAL MODEL

A steady, two-dimensional, incompressible stagnation point flow over a stretching sheet aligned along the horizontal direction is considered. The flow involves a hybrid nanofluid based on polystyrene. The fluid is subjected to a constant magnetic field of strength  $B_0$ , applied normally to the sheet as shown in Fig. 1. The temperature  $T_w$ , and concentration  $C_\infty$  on the sheet are

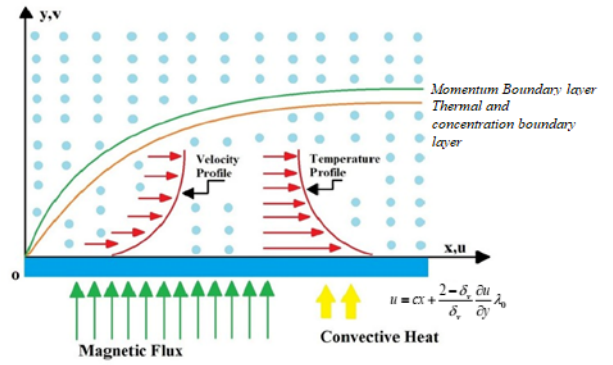


FIG. 1: Geometry of the flow problem.

assumed to be constant and higher than the ambient values  $T_\infty$ , and  $C_\infty$  respectively. The governing equations for the flow are derived from the principles of continuity, momentum, energy, and mass transfer within the boundary layer approximation. These equations are expressed as follows:

$$\frac{\partial u}{\partial x} + \frac{\partial v}{\partial y} = 0 \quad (1)$$

$$u \frac{\partial u}{\partial x} + v \frac{\partial u}{\partial y} = \frac{\mu_{hnf}}{\rho_{hnf}} \frac{\partial^2 u}{\partial y^2} + u_e \frac{\partial u_e}{\partial x} - \frac{\sigma_{hnf} B_0^2}{\rho_{hnf}} \left( u - u_e - \lambda_1 r \frac{\partial u}{\partial y} \right) - \frac{\mu_{hnf}}{\rho_{hnf}} \frac{u}{k^*} - \lambda \left[ u^2 \frac{\partial^2 u}{\partial x^2} + v^2 \frac{\partial^2 u}{\partial y^2} + 2uv \frac{\partial^2 u}{\partial y \partial x} \right] \quad (2)$$

$$u \frac{\partial T}{\partial x} + v \frac{\partial T}{\partial y} = \frac{K_{hnf}}{(\rho C_p)_{hnf}} \left( \frac{\partial^2 T}{\partial y^2} \right) + \frac{\mu_{hnf}}{(\rho C_p)_{hnf}} \left( \frac{\partial u}{\partial y} \right)^2 + \frac{Q_0}{(\rho C_p)_{hnf}} (T - T_\infty) \quad (3)$$

$$v \frac{\partial C}{\partial y} + u \frac{\partial C}{\partial x} = D_m \frac{\partial^2 C}{\partial y^2} - K_r^2 \left( \frac{T}{T_\infty} \right)^m \exp \left[ -\frac{E_a}{KT} \right] (C - C_\infty) \quad (4)$$

Here, the electrical conductivity is represented by

$\sigma_{hnf}$ ,  $\lambda$ , and  $Q_0$  the fluid relaxation time. The boundary conditions are set as follows:

$$u = cx + \frac{2 - \delta_v}{\delta_v} \frac{\partial u}{\partial y} \lambda_0, \quad C = C_w, \quad v = v_w, \quad h_f(T - T_w) = -K_{hnf} \frac{\partial T}{\partial y} \quad \text{at } \eta = 0 \quad (5)$$

$$u \rightarrow u_e = ax, \quad C \rightarrow C_\infty, \quad T \rightarrow T_\infty \quad \text{as } \eta \rightarrow \infty \quad (6)$$

For the conversion of the above dimensional PDEs, the following similarity variables are proposed:

$$\eta = y \sqrt{\frac{c}{v_f}}, \quad v = -f(\eta) \sqrt{cv_f}, \quad u = cx f'(\eta), \quad u_e = ax, \quad \theta(\eta) = \frac{T - T_\infty}{T_w - T_\infty}, \quad \phi(\eta) = \frac{C - C_\infty}{C_w - C_\infty} \quad (7)$$

After simplification, we come forth with the following

set of ordinary differential equations:

$$f''' - A_1 (f'^2 - f f'') - M A_4 (f' - D - E f'') - K_p f' - A_1 \beta (f''' f^2 - 2 f' f'' f) + A_1 D^2 = 0 \quad (8)$$

$$\theta'' + \frac{k_f}{k_{hnf}} \text{Pr} (A_3 f \theta' + E c A_4 f''^2 + Q \theta) = 0 \quad (9)$$

$$\phi'' + S c f \phi' - \sigma S c (1 + \delta \theta)^n \exp\left(\frac{-E}{1 + \delta \theta}\right) \phi = 0 \quad (10)$$

The transformed boundary conditions are:

$$s_1 = f(\eta), \quad f'(\eta) = 1, \quad B_i(1 - \theta(\eta)) = \frac{k_{hnf}}{k_f} \theta'(\eta), \quad \phi(\eta) = 1, \quad \text{at } \eta = 0 \quad (11)$$

$$f'(\infty) \rightarrow 0, \quad \theta(\infty) \rightarrow 0, \quad \phi(\infty) \rightarrow 0, \quad \text{as } \eta \rightarrow \infty \quad (12)$$

Different dimensionless variables in the above equations are defined as:

$$\left. \begin{aligned} \beta = \lambda c, \quad \frac{\sigma B_0^2}{\rho_f c} = M, \quad K_p = \frac{\nu_f}{ck_*}, \quad \text{Pr} = \frac{\nu_f(\rho C_p)_f}{k_f}, \quad Ec = \frac{c^2 x^2}{(C_p)_f(T_w - T_\infty)}, \quad D^2 = \frac{a^2}{c^2}, \quad E = \frac{Ea}{kT_\infty}, \\ Q = \frac{Q_0}{c(\rho C_p)_{hnf}}, \quad S = \frac{\nu_w}{\sqrt{c\nu_f}}, \quad Bi = \frac{h}{k_f} \sqrt{\frac{\nu_f}{c}}, \quad D = \frac{a}{c}, \quad \sigma = \frac{kr^2}{c}, \quad \delta = \frac{T_w - T_\infty}{T_\infty}, \quad Sc = \frac{\nu_f}{D}, \quad E_1 = \lambda_1 r \sqrt{\frac{c}{\nu_f}}. \end{aligned} \right\} \quad (13)$$

Also:

$$\left. \begin{aligned} (1 - \varphi_1)^{2.5}(1 - \varphi_2)^{2.5} \left[ (1 - \varphi_2)(1 - \varphi_1) + \varphi_1 \frac{\rho_{s1}}{\rho_f} + \varphi_2 \frac{\rho_{s2}}{\rho_f} \right] &= A_1, \\ (1 - \varphi_2)(1 - \varphi_1) + \varphi_1 \frac{\rho_{s1}}{\rho_f} + \varphi_2 \frac{\rho_{s2}}{\rho_f} &= A_2, \\ (1 - \varphi_2)(1 - \varphi_1) + \varphi_1 \frac{(\rho C_p)_{s1}}{(\rho C_p)_f} + \varphi_2 \frac{(\rho C_p)_{s2}}{(\rho C_p)_f} &= A_3, \\ (1 - \varphi_1)^{2.5}(1 - \varphi_2)^{2.5} &= A_4, \\ \frac{k_{hnf}}{k_f} = \frac{k_{s2} + (s_f - 1)k_{bf} - (s_f - 1)\varphi_2(k_{bf} - k_{s2})}{k_{s2} + (s_f - 1)k_{bf} + \varphi_2(k_{bf} - k_{s2})} \cdot \frac{k_{s1} + (s_f - 1)k_f - (s_f - 1)\varphi_1(k_f - k_{s1})}{k_{s1} + (s_f - 1)k_f + \varphi_1(k_f - k_{s1})} &= A_5. \end{aligned} \right\} \quad (14)$$

### A. NUMERICAL SOLUTION

With the help of shooting method, the non-linear system of the governing ODE's Eqs. (8), (9), (10), (11), and (12) are solved. The Runge-Kutta approach is used

to develop computational coding in MATLAB scripts. The higher order derivative must be converted into a 1st order differential system. Seven first order ODE's are produced using the following symbols.

$$f = y_1, \quad f' = y_2, \quad f'' = y_3, \quad \theta = y_4, \quad \theta' = y_5, \quad \varphi = y_6, \quad \varphi' = y_7 \quad (15)$$

Seven first order ODE's is used to convert momentum,

heat and concentration equations with conditions are shown below:

$$\left. \begin{aligned} y'_1 &= y_2, \quad y'_2 = y_3, \\ y'_3 &= \frac{1}{(1 - A_1\beta y_1^2)} \left( A_1(y_2^2 - y_1 y_3) + A_4 M(y_2) + K_p y_2 + 2A_1\beta y_1 y_2 y_3 \right), \\ y'_4 &= y_5, \quad y'_5 = -\frac{k_f}{k_{hnf}} \text{Pr} \left( A_3 y_1 y_5 + Ec A_4 y_2^2 + Q y_4 \right), \\ y'_6 &= y_7, \quad y'_7 = \sigma Sc (1 + \delta y_4)^n \exp\left(\frac{-E}{1 + \delta y_4}\right) y_6 - Sc y_1 y_7. \end{aligned} \right\} \quad (16)$$

Along:

$$\left. \begin{aligned} y_1(0) = s_1, \quad y_2(0) = 1, \quad B_i(1 - y_4(0)) = \frac{k_f}{k_{hnf}} y_5(0), \quad y_6(0) = 1, \quad \text{at } \eta = 0, \\ y_2(\infty) \rightarrow 0, \quad y_4(\infty) \rightarrow 0, \quad y_6(\infty) \rightarrow 0, \quad \text{as } \eta \rightarrow \infty. \end{aligned} \right\} \quad (17)$$

### III. RESULTS AND DISCUSSION

Numerical solutions have been determined for two fluid flow scenarios: (a) GO/ polystyrene (simple nanofluid) and (b) GO + Ag/ polystyrene (hybrid nanofluid). These solutions focus on analyzing key physical quantities such as the Prandtl number, magnetic parameter, permeability parameter, Eckert number, heat generation parameter, and Schmidt number. The validity of the results is confirmed by comparing them with earlier data in Table 1 for the Prandtl number under specific conditions, demonstrating reliable agreement.

TABLE I: : Comparison for the values of Pr while the remaining parameters are zero.

Pr	Gorla and Sidawi [14]	Khan and Pop [15]	Wang [16]	Our Results
2.0	0.9114	0.9113	0.9114	0.91115
6.13	-	1.75950	-	1.75951
20.0	3.3539	3.3539	3.3539	3.35381

According to Figs. 2 and 3, the non-dimensional velocity  $f'(\eta)$  diminishes dramatically when the magnetic parameter  $M$  and the porosity parameter  $K_p$  rises. The progressive resistive force is called the Lorentz force due to the increasing magnetic parameters produced, which resists the fluid movement and ultimately slows down the motion of the fluid. Like this, the permeability of porous media is inversely related to the velocity profile, so a higher permeability indicates a greater barrier to fluid flow caused by the porous structure.

When the Maxwell fluid parameter  $\beta$  and the suction parameter  $s_1$  are reduced, the fluids flow more quickly, as seen in Figs.4 and 5, respectively. The Maxwell fluid parameter defines the non-Newtonian behavior of the fluid. Higher values of  $\beta$  will make the fluid denser, and it behaves thinner when the values of the Maxwell fluid parameter get lower. Due to the thinner behavior of the fluid for the decreasing values of  $\beta$ , the fluid motion increases. The same phenomenon occurs for the suction parameter Suction or injection is produced due to the pores on the sheet. Higher values of the suction parameter indicate a greater number of pores on the sheet, which ultimately make an influential impact on the velocity of the working fluid. In Fig. 5, when the permeability of the medium reduces, the fluid moves more quickly.

Fluid's temperature significantly increased with an in-

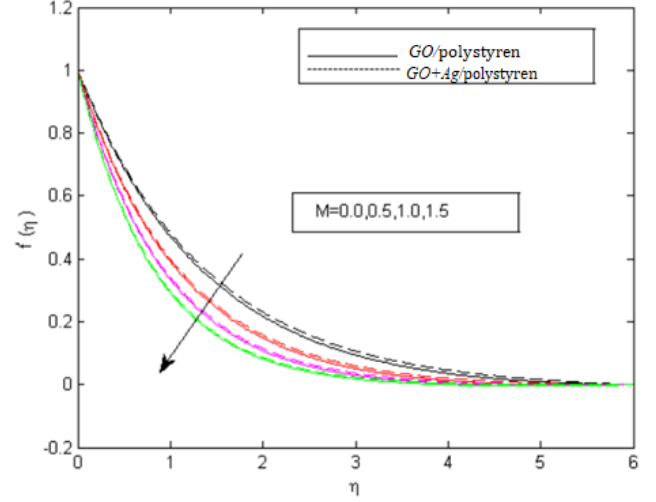


FIG. 2: Influence of  $M$  on  $f'(\eta)$ .

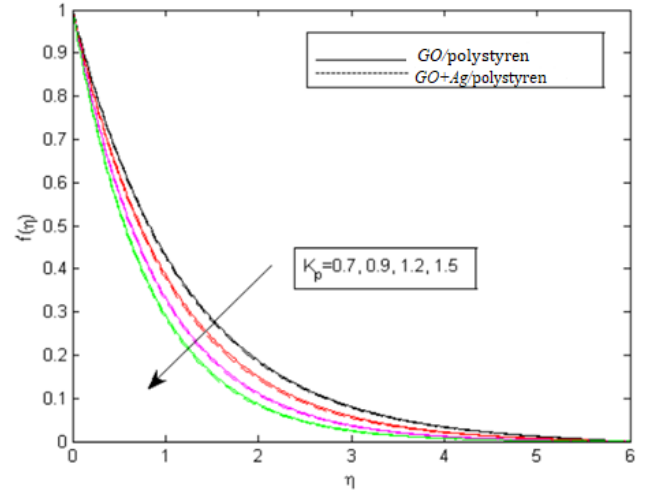


FIG. 3: Influence of  $K_p$  on  $f'(\eta)$ .

crease in the volume fraction  $\phi_2$  as seen in Fig. 6. A higher volume fraction of nanoparticles in the base fluid will enhance the thermal conductivity of the fluid. That increment in the thermal conductivity will ultimately enhance the temperature of the fluid. The impact of power index  $n$  on the concentration profile is displayed

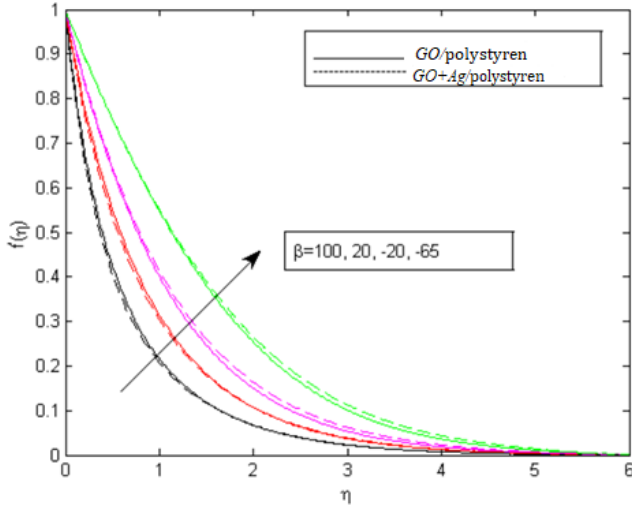


FIG. 4: Influence of  $\beta$  on  $f'(\eta)$ .

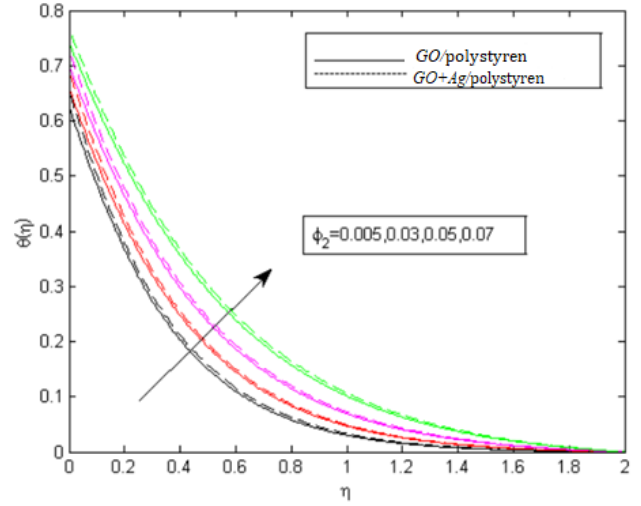


FIG. 6: : Influence of  $\phi_2$  on  $\theta(\eta)$ .

in Fig. 7. The term  $\sigma(1 + \delta\theta)^n \exp\left(\frac{-E}{1 + \delta\theta}\right)$  in the concentration equations amplifies with a magnification in ( $\sigma$ ) or ( $n$ ) which encourages the destructive chemical reaction. Hence, a higher value of  $n$  depreciates the mass fraction field.

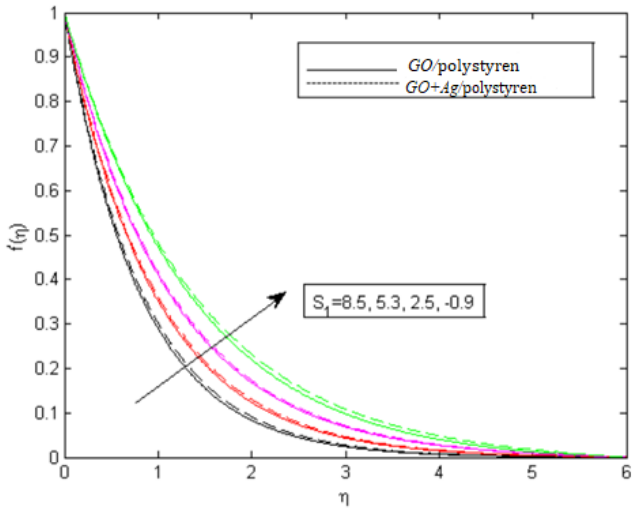


FIG. 5: Influence of  $S_1$  on  $f'(\eta)$ .

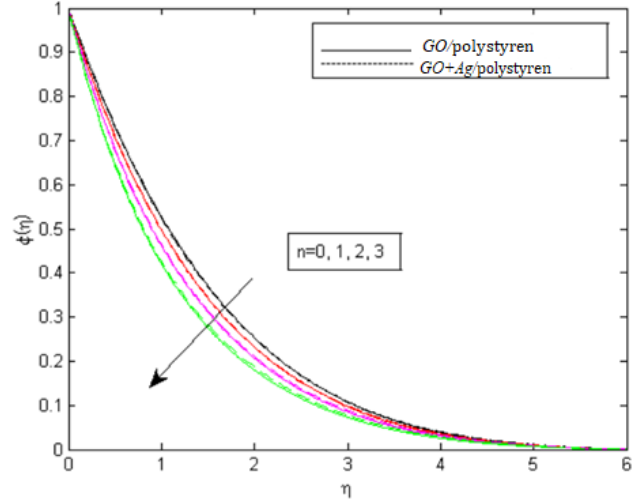


FIG. 7: Impact of  $n$  on  $\phi(\eta)$  .

#### IV. CONCLUSION

Theoretically, in this work, heat transfer using hybrid nanofluid flow is brought on a linear stretchy sheet. In the polystyrene, graphene oxide (Go) is hybridized with

(Ag) silver nanoparticles. The problem is tackled with the help of the shooting method. Coding is done on MATLAB software. The influence of magnetic field, heat source, and activation energy is also taken into account. The main findings of the present work are as follows:

1. The magnitude of  $f''(0)$  is reduced by increasing the values of  $\beta$ , and  $s_1$ , and the skin friction coefficient grows with the  $M$  and  $K_p$ .
2. Nusselt number  $\theta'(0)$  exhibits progressive behavior for increasing Prandtl numbers, and it shows an inverse

relationship to  $Q$  and  $Ec$ .

3. Higher concentration of Ag particles in the base fluid will resultantly enhance the temperature of the working fluid.

4. The Biot number plays a vital role in thermal analysis. When the Biot number  $Bi$  is escalated, the temperature rises.

5. The mass transfer declines with the increasing values of the Schmidt number.

6. It is noted through calculations that an average of 16 % increase in the rate of heat transfer over the sheet is observed in the presence of a hybrid nanofluid.

## DECLARATION OF COMPETING INTEREST

The authors declare that they have no known competing financial interests or personal relationships that could have appeared to influence the work reported in this paper.

## ACKNOWLEDGMENTS

We are pleased to acknowledge “1st International Conference on Sciences for Future Trends (ICSFT)-University of Lahore, Sargodha”, for providing a valuable platform for sharing this research.

## REFERENCES

- <sup>1</sup>T. Sajid, M. Bilal, and G. C. Altamirano, “Cattaneo-christov model for cross nanofluid with sores and dufour effects under endothermic/exothermic reactions: a modified buongiorno tetra-hybrid nanofluid approach,” *Z Angew Math Mech* (2024), doi: [10.1002/zamm.202300044](https://doi.org/10.1002/zamm.202300044), e202300044.
- <sup>2</sup>Y. Mehmood, A. Alsinai, A. U. K. Niazi, M. Bilal, and T. Akhtar, “Numerical study of maxwell nanofluid flow with mwnt and swcnt considering quartic autocatalytic reactions and thompson troian slip mechanism,” *Discover Applied Sciences* **6**, 534 (2024).
- <sup>3</sup>M. Bilal, T. Ishfaq, S. A. Lone, and Y. Mehmood, “A numerical simulation of the unsteady mhd nanofluid flow over a rotating disk in a porous medium with uniform suction and convective effects,” *International Journal of Ambient Energy* **45**, 2410924 (2024).
- <sup>4</sup>M. Bilal, S. A. Lone, S. Anwar, S. S. and S. Fatima, M. Ramzan, and M. Nadeem, “An exact solution for the entropy base flow of electroosmotic magneto-nanofluid through microparallel channel,” *International Journal of Modern Physics B* (2023), <https://doi.org/10.1016/j.appt.2016.12.005>.
- <sup>5</sup>M. Nadeem, I. Siddique, M. Bilal, and K. Anjum, “Numerical study of mhd prandtl eyring fuzzy hybrid nanofluid flow over a wedge,” *Numerical Heat Transfer, Part A: Applications* (2023), <https://doi.org/10.1080/01430750.2024.2410924>.
- <sup>6</sup>M. D. Shamshuddin, A. Saeed, S. R. Mishra, R. Katta, and M. R. Eid, “Homotopic simulation of mhd bioconvective flow of water-based hybrid nanofluid over a thermal convective exponential stretching surface,” *International Journal of Numerical Methods for Heat and Fluid Flow* **34**, 31–53 (2024).
- <sup>7</sup>R. R. Kairi, S. Shaw, S. Roy, and S. Raut, “Thermosolutal marangoni impact on bioconvection in suspension of gyrotactic microorganisms over an inclined stretching sheet,” *Journal of Heat Transfer* **143** (2021), <https://doi.org/10.1016/j.euromechflu.2022.09.004>.
- <sup>8</sup>R. Roy, S. Raut, and R. R. Kairi, “Thermosolutal marangoni bioconvection of a non-newtonian nanofluid in a stratified medium,” *Journal of Heat Transfer* **144** (2022), <https://doi.org/10.1115/1.4054770>.
- <sup>9</sup>S. Roy and R. R. Kairi, “Bio-marangoni convection of maxwell nanofluid over an inclined plate in a stratified darcy–forchheimer porous medium,” *Journal of Magnetism and Magnetic Materials* **572** (2023), <https://doi.org/10.1016/j.jmmm.2023.170581>.
- <sup>10</sup>M. B. Rekha, I. E. Sarris, J. K. Madhukesh, K. R. Raghunatha, and B. C. Prasannakumara, “Activation energy impact on flow of aa7072-aa7075/water-based hybrid nanofluid through a cone, wedge and plate,” *Micromachines* **13**, 302 (2022).
- <sup>11</sup>I. Ullah, R. Ali, H. Nawab, I. Uddin, T. Muhammad, and I. Khan, “Theoretical analysis of activation energy effect on prandtl-eyring nanoliquid flow subject to melting condition,” *J Non-Equilib Thermodyn* **47**, 1–12 (2022).
- <sup>12</sup>M. Dhlamini, P. K. Kameswaran, P. Sibanda, S. Motsa, and H. Mondal, “Activation energy and binary chemical reaction effects in mixed convective nanofluid flow with convective boundary conditions,” *J Comput Des Eng* **6**, 149–158 (2019).
- <sup>13</sup>M. I. Khan and F. Alzahrani, “Activation energy and binary chemical reaction effect in nonlinear thermal radiative stagnation point flow of walter-b nanofluid: numerical computations,” *Int J Mod Phys B* **34**, 2050132 (2020).
- <sup>14</sup>R. S. Gorla and I. Sidawi, “Free convection on a vertical stretching surface with suction and blowing,” *Appl. Sci. Res.* **52**, 247–257 (1994).
- <sup>15</sup>C. Y. Wang, “Stagnation flow towards a shrinking sheet,” *Int J Nonlinear Mech.* **43**, 377–382 (2008).
- <sup>16</sup>W. A. Khan and I. Pop, “Boundary-layer flow of a nanofluid past a stretching sheet,” *Int. J. Heat Mass Trans.* **53**, 2477–2483 (2010).